RSC Advances

PAPER

View Article Online
View Journal | View Issue

Cite this: *RSC Adv.*, 2020, **10**, 11643

Anionic structural effect on the dissolution of arabinoxylan-rich hemicellulose in 1-butyl-3-methylimidazolium carboxylate-based ionic liquids†

Qi Xia,[ab] Hong Peng,*[ab] Lin Yuan,[ab] Lifang Hu,[ab] Yu Zhang[ab] and Roger Ruan[ab]

The exploration of a highly efficient and environment-friendly solvent for dissolving hemicellulose is significant. In this study, 1-butyl-3-methylimidazolium carboxylate ([Bmim]carboxylate)-based ionic liquids (ILs), including [Bmim]formate, [Bmim]acetate, [Bmim]propionate, and [Bmim]butyrate, were used as solvents to dissolve arabinoxylan-rich hemicellulose from bamboo. The hemicellulose solubility in the ILs was determined as a function of temperature. The interaction between the hemicellulose and the ILs was evaluated by using ^{1}H and ^{13}C NMR techniques. The hemicelluloses regenerated from the saturated IL solutions were characterized. Results showed that the temperature and structure of carboxylate anions deeply affected the hemicellulose solubility. The carboxylate anion played a more important role than the imidazolium cation in hemicellulose dissolution. The hydrogen bond that formed between the ILs and the hydroxyl groups at the XC2 position of xylopyranose units of hemicellulose was stronger than that between the ILs and the hydroxyl groups at XC3 position of xylopyranose units. The hydrogen bond strength between the hemicellulose and the ILs was affected by the alkyl chain of the carboxylate anion and the hemicellulose concentration. The disruption of the inter- and intra-molecular hydrogen bonds in hemicellulose by the ILs was responsible for the hemicellulose dissolution. The main chain of hemicellulose remained nearly unchanged during the dissolution process.

Received 3rd December 2019
Accepted 15th March 2020

DOI: 10.1039/c9ra10108j

rsc.li/rsc-advances

Introduction

Renewable biomass has become the focus of researchers worldwide to resolve the increasingly deteriorating environment and energy crisis.[1] Lignocellulosic biomass, which is an important renewable biomass on earth, is mainly composed of hemicellulose, cellulose, and lignin.[1] Hemicellulose, which is mainly composed of xylose, arabinose, galactose, glucose, mannose, uronic acid, *etc.*,[2] is an important heterogeneous polysaccharide in plant cell walls and contributes approximately 20–40% to the whole plant cell wall.[1,3,4] Hemicellulose can be successfully conversed into biofuels,[5,6] materials,[7,8] chemicals,[9,10] and functional food ingredients.[11,12] However, hemicellulose does not dissolve in many conventional solvents. Consequently, the progress of hemicellulose utilization and conversion is hindered. The existing dissolution techniques, such as alkaline solvent system and hydrothermal method, usually cause environmental problems and hemicellulose degradation.[13–15] Therefore, a highly efficient and environment-friendly solvent system for dissolving hemicellulose is necessary.

Ionic liquids (ILs) have potential for lignocellulosic biomass dissolution as a new class of green solvent because of their excellent physicochemical properties, such as thermally stable, low melting point, low volatility, recyclability, and tunable chemical structure.[16–18] ILs has attracted great attention for fractionating lignocellulosic biomass.[19,20] However, the dissolution of hemicellulose in ILs and interaction with ILs are still unclear because of its structural complexity in the plant cell wall. Consequently, the rational selection of ILs for fractionating hemicellulose from lignocellulosic biomass is blocked. Therefore, elucidating the dissolution of hemicellulose in ILs and its interaction with ILs is imperative for selecting highly efficient ILs to dissolve hemicellulose.

However, most dissolution mechanisms focus on cellulose and lignin in ILs.[21–24] Nevertheless, few studies have reported the dissolution behavior of hemicellulose in ILs.[10,25–28] Peng *et al.* found that xylan-rich hemicellulose (XH), which has two hydroxyl groups in its sugar units, can form the electron donor–electron acceptor complexes with 1-butyl-3-methylimidazolium chloride ([Bmim]Cl); XH (concentration of 2.5 wt%) can be

[a]*Engineering Research Center of Biomass Conversion, Ministry of Education, Nanchang University, Nanchang, Jiangxi 330047, P. R. China. E-mail: penghong@ncu.edu.cn*

[b]*State Key Laboratory of Food Science and Technology, Nanchang University, Nanchang, Jiangxi 330031, P. R. China*

† Electronic supplementary information (ESI) available. See DOI: 10.1039/c9ra10108j

completely dissolved in [Bmim]Cl at 90 °C within 90 min.[25] The interaction between the hydroxyl group of XH and [Bmim]Cl was crucial for the XH dissolution in [Bmim]Cl and the subsequent esterification with maleic anhydride.[25] The results obtained by Matsagar *et al.* indicated that the ion–dipole-type interactions of the alkyl imidazolium groups and hydrogen sulfate ions of Brösted acidic ionic liquids (BAIL) with hydroxyl groups of hemicellulose, which was proposed by the ^{1}H NMR technique, helps achieve excellent BAIL catalytic activity for the hemicellulose hydrolysis.[10] 1-Butyl-3-methylimidazolium acetate ([Bmim]acetate) exhibits stronger ability to dissolve hemicellulose from the cell wall of *Eucalyptus* than [Bmim]Cl.[26] Moyer *et al.* suggested that the strong interaction between the 1-allyl-3-methylimidazolium formate ([Amim]formate) and the hemicellulose is an important factor enhancing the solubility of the hybrid polar in the IL under mild conditions based on the solubility, Kamlet–Taft parameters, and molecular dynamic simulations.[27] The cationic and anionic properties of ILs are all important in explaining solvent–solute interactions between the ILs and the hemicellulose.[27] The above-mentioned studies revealed some important information for the hemicellulose dissolution in ILs. However, no systematic attempt has been carried out to elucidate the effect of the chemical structure of ILs on the solubility of hemicellulose in ILs and the interaction between the hemicellulose and the ILs.

In this work, the effect of the carboxylate structure on the dissolution of arabinoxylan-rich hemicellulose from bamboo in ILs when the cation was kept fixed as 1-butyl-3-methylimidazolium ([Bmim]$^{+}$) was investigated. The hemicellulose solubility in the ILs was determined as a function of temperature. ^{1}H and ^{13}C NMR techniques were used to characterize the mixture of hemicellulose and ILs in DMSO-d_6 to reveal the interactions leading to the difference in solubility. The effect of hemicellulose concentration on the interaction between the hemicellulose and the ILs was discussed. The hemicellulose was regenerated from the saturated IL solution and then characterized and compared with the original hemicellulose to examine the physicochemical change.

Results and discussion

Solubility of the bamboo hemicellulose in the Ils

The solubilities of the bamboo hemicellulose in the four ILs at the temperature ranging from 30 °C to 150 °C were given in Fig. 1. The hemicellulose solubility in the ILs increased with increasing temperature in the range 30–150 °C. The high solubilities, which were obtained at 150 °C in [Bmim]formate, [Bmim]acetate, [Bmim]propionate, and [Bmim]butyrate, were 4.79, 15.56, 2.27, and 3.84 g/100 g IL, respectively. The hemicellulose solubility was greatly affected by temperature when the temperature was higher than 80 °C. For example, the hemicellulose solubility in [Bmim]acetate at 150 °C was 15.56 g/100 g IL, which was nearly 16 times that obtained at 80 °C (0.96 g/100 g IL). Therefore, the hydrogen bonds in the hemicellulose can be partially be disrupted at high temperature.[29]

As shown in Fig. 1, the hemicellulose solubility in the four types of ILs was in the following order: [Bmim]acetate > [Bmim]formate > [Bmim]butyrate > [Bmim]propionate. [Bmim]formate, [Bmim]propionate, and [Bmim]butyrate had moderate solvation ability for bamboo hemicelluloses. By contrast, [Bmim]acetate exhibited much stronger solvation ability than the other three ILs. The highest solubilities of hemicelluloses in [Bmim]acetate were 3.25, 6.85, and 4.05 times those in [Bmim]formate, [Bmim]propionate, and [Bmim]butyrate, respectively. The results obtained by Zhang *et al.* indicated that the replacement of H in HCOO– anion by electron-donating groups, such as CH_3, CH_2CH_3, and $CH_2CH_2CH_3$, would increase hemicellulose solubility.[30] However, the solubility values showed in Fig. 1 did not follow this rule. This phenomenon was due to the presence of steric hindrance, which affected the interaction between the hemicellulose and the ILs. In theory, the steric hindrance of [Bmim]butyrate was stronger than that of [Bmim]acetate and weaker than that of [Bmim]propionate because of the even-odd rule of the carbon number in alkyl chain of carboxylate anion. The influence of steric hindrance of alkyl chain on the solubility was stronger than that of the electron-donating effect of alkyl chain among [Bmim]acetate, [Bmim]butyrate, and [Bmim]propionate. At the same time, the hydrophobicity of these four ILs theoretically increased as the alkyl chain length of carboxylate anion increased,[31] resulting possibly in the decrease of solvability for hemicellulose. Finally, the increase of the alkyl chain length of carboxylate anion could lead to the increase of viscosity, which hindered the mass transfer and inhibited the dissolution of hemicelluloses.[32] Considering the same cation of 1-butyl-3-methyl imidazolium ([Bmim]$^{+}$), this result suggested that the hemicellulose solubility strongly depended on the variation of the alkyl chain length in the anions of the ILs.

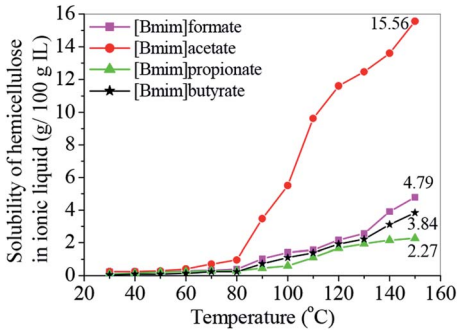

Fig. 1 Solubility of hemicellulose in the ILs as a function of temperatures.

The above-mentioned results showed that the rational selection of IL solvents for efficient extraction of hemicellulose from lignocellulosic biomass and hemicellulose dissolution for further reaction is necessary. One principle that should be considered is as follows: the alkyl chain of anion of ILs with exact electron-donation but without bulky steric hindrance groups should be given top priority.

NMR analysis of the mixture of hemicellulose and ILs

^{1}H and ^{13}C NMR techniques were used to analyze the mixtures of hemicellulose and ILs. This step was conducted to deeply

understand the dissolution mechanism of hemicellulose in the ILs. The schematic structure and numbering of the ILs and bamboo hemicellulose which mainly consists of arabinoxylans[2] are given in Fig. 2. The relative chemical shift changes of the chemical shifts ($\Delta\delta$) of protons and carbons referring to the pure hemicellulose and ILs were calculated according to eqn (1) and (2), respectively. The ^{1}H and ^{13}C NMR spectra of the pure ILs and original hemicellulose are shown in Fig. S1 and S2,† respectively. The ^{1}H and ^{13}C NMR spectra of the mixtures of 10 wt% hemicellulose and ILs are given in Fig. S3 and S4.† As shown in Fig. S2e,† the five major peaks at 102.22, 73.08, 74.48, 75.82, and 63.75 ppm were attributed to XC1, XC2, XC3, XC4, and XC5, respectively.[25,28] The $\Delta\delta$ values of ^{13}C and ^{1}H chemical shifts of ILs, xylopyranose unit in hemicelluloses, and DMSO-d_6 after dissolving 10 wt% hemicellulose in the ILs are shown in Fig. 3.

As illustrated in Fig. 3a and b, the $\Delta\delta$ values of almost all carbons and protons (except C2 and C2–H of all ILs, C6 and C7 of IL_2, and C4–H and C5–H of IL_2) in the 1-butyl-3-methylimidazolium cation could be neglected (-0.05 ppm $< \Delta\delta <$ 0.05 ppm). This notion suggests that the chemical shifts of these carbons and protons did not change or only slightly changed after mixing ILs with 10 wt% hemicellulose. The decreasing chemical shifts of C2 and C2–H atoms ($\Delta\delta < 0.00$ ppm) in the imidazolium ring indicated that the carbon and proton chemical shifts at the 2-position moved to a higher field after mixing ILs with 10 wt% hemicellulose. This phenomenon was due to the disrupted interaction between the acidic C2–H proton and the carboxylate anion of ILs by hemicellulose. Such situation leads to the formation of a new hydrogen bond between the acidic C2–H proton and the hydroxyl oxygen atom in hemicellulose. Accordingly, the electron cloud density around the C2 and C2–H atoms increased, thereby leading to an upfield shift and decrease of chemical shifts.[29,33] The extents of the chemical shift changes of C2 and C2–H were much higher than those of C4, C4–H, C5, and C5–H (Fig. 3a and b). C2–H showed a stronger acidity than C4–H and C5–H. Thus, the hemicellulose molecule interacted with the acidic protons in the imidazolium cation. The ability to form a hydrogen bond with hemicellulose is strong with a strong proton acidity. The significant increase of the carboxyl C11 atom in the carboxylate anion of ILs revealed that the oxygen atom of carboxylate anion,

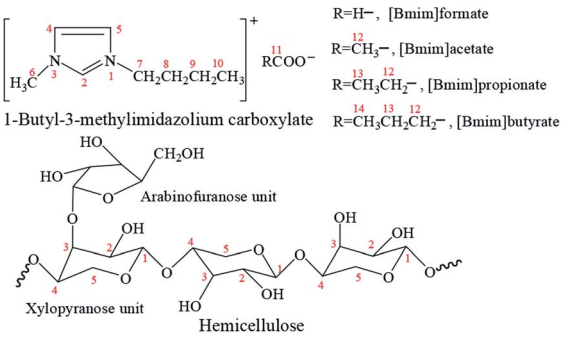

Fig. 2 Schematic structures, numbering, and abbreviations of ILs and bamboo hemicellulose.

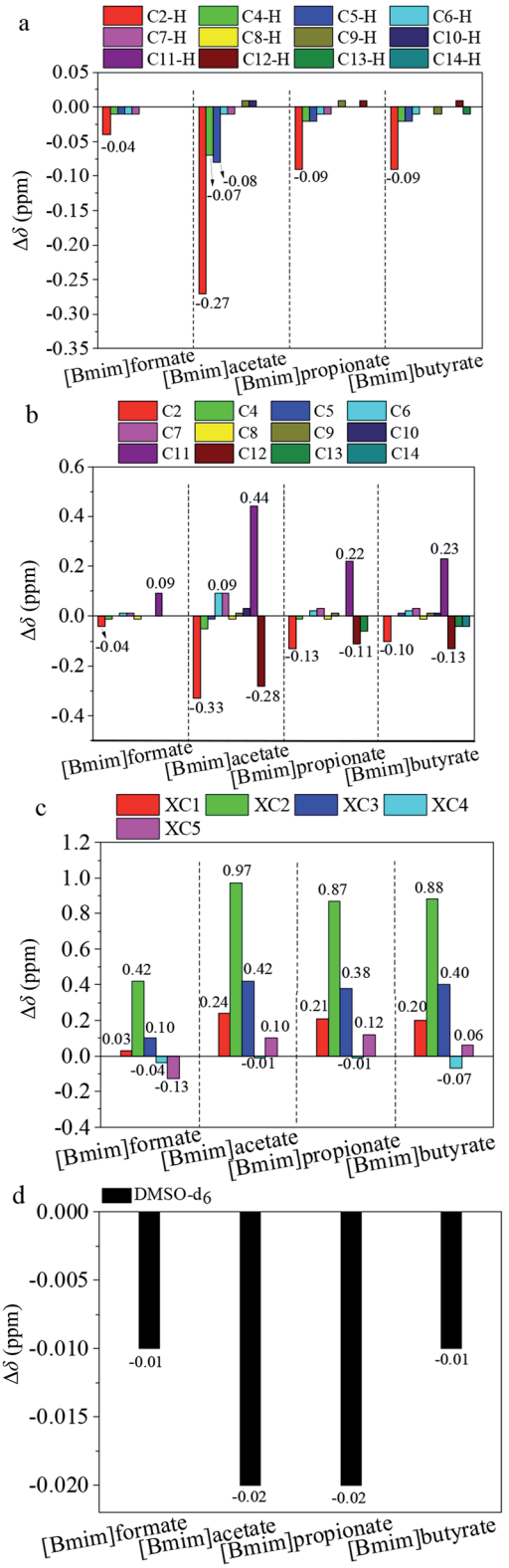

Fig. 3 Relative change of the ^{13}C and ^{1}H chemical shifts (δ/ppm) of (a) and (b) ILs, (c) xylopyranose unit in hemicelluloses, and (d) DMSO-d_6 after dissolving 10 wt% hemicellulose in the ILs.

which acted as a hydrogen bond acceptor, most probably interacted with the hydroxyl proton in hemicellulose through a hydrogen bond, thereby leading to the downfield movement of

the chemical shift and an increase of chemical shifts (Fig. 3b).[29,30,33] The absolute changes of ^{13}C chemical shift $|\Delta\delta|$ of C11 were higher than the corresponding values of C2. The hydrogen bond strength between the carboxylate anion and the hydroxyl oxygen proton in the hemicellulose was stronger than that between C2–H of imidazolium cation and hydroxyl oxygen atom in hemicellulose. Specifically, the cation and anion of the ILs played important role in the hemicellulose dissolution in the ILs. However, the anion performed a predominant role. The signals of C12, C13, and C14 moved upfield due to the weakened electron-withdrawing capacity of COO^- toward alkyl in the carboxylate anion caused by the hydrogen bonding interaction between anion and hydroxyl proton in hemicellulose (Fig. 3b).[30]

Fig. 3c demonstrates that the chemical shifts of carbons of the xylopyranose unit in the hemicellulose also changed after dissolving 10 wt% hemicellulose in the ILs. The signals of the XC2 and XC3 atoms significantly moved downfield. This occurrence was due to the hydrogen bonding interaction that occurred between the imidazolium cation or the carboxylate anion and the hydroxyl at the positions of XC2 and XC3 of the xylopyranose unit in the hemicellulose during the hemicellulose dissolution in the ILs;[23,30,33] such a condition decreased the electron cloud density around the corresponding XC2 and XC3 atoms and increased the chemical shifts.[29,33,34] Fig. 3c exhibits that the downfield shift extent of XC2 was greater than that of XC3. This finding indicated that the hydrogen bond strength between XC2–OH and ILs was stronger than that between XC3–OH and ILs. The chemical shift changes of XC1, XC4, and XC5 were due to the redistribution of the electron cloud density on the xylopyranose ring.[29] Fig. 3d shows the relative changes of carbon chemical shifts of DMSO-d_6. The $\Delta\delta$ values of ^{13}C chemical shifts of DMSO-d_6 could also be neglected (-0.05 ppm $< \Delta\delta < 0.05$ ppm). It suggested that there was no synergistic interaction occurred with DMSO-d_6. The deuterated solvent only performed the function of solvent and mainly served to dissociate the ion pairs in ILs into solvated cations and anions.[35]

Fig. 1 and 3 show that the law of hemicellulose solubility in the ILs was nearly in accordance with those of the absolute chemical shift changes of C2, C2–H, XC2, and XC3, except [Bmim]formate. Although the hemicellulose solubility in [Bmim]formate was slightly higher than those in [Bmim] propionate and [Bmim]butyrate. The absolute chemical shift changes of C2, C2–H, XC2, and XC3 of [Bmim]formate were smaller than those of [Bmim]propionate and [Bmim]butyrate. The reason was still unclear. In summary, the relative chemical shift of C2, C2–H, XC2, and XC3 is strong, and the hemicellulose solubility that could be obtained is high, when the hydrogen bonding interaction between the hemicellulose and the ILs is strong. The hydrogen bond formation between the hemicellulose and the ILs led to the disruption of the inter- and intra-hydrogen bonds in hemicellulose. This circumstance resulted in the hemicellulose dissolution in ILs.

The results shown in Fig. 1 and 3 demonstrate that [Bmim] acetate had a strong ability to dissolute the bamboo hemicellulose, which consists of arabinoxylans.[2] Thus, [Bmim] acetate was chosen as the representative IL to determine the effect of various hemicellulose concentrations (10, 20, 30, 40, and 50 wt%) on the interaction between the hemicellulose and the ILs. The NMR spectra of the mixture of hemicellulose and [Bmim]acetate are given in Fig. S3–S6.† The $\Delta\delta$ data are summarized in Fig. 4.

As illustrated in Fig. 4a and b, the $\Delta\delta$ values of C2–H, C4–H, C5–H, C2, C11, and C12 atoms of [Bmim]acetate significantly changed with the increase of the hemicellulose concentration. The $|\Delta\delta|$ values increased with the increase of the hemicellulose concentration. This occurrence was due to C2–H, C4–H, C5–H, and carboxylate anion that were attracted by more hydroxyl groups from the hemicellulose with the increase of the hemicellulose concentration. Accordingly, a strong interaction (hydrogen bond) between [Bmim]acetate and hemicellulose was formed, leading to additional extensive downfield or upfield shifts. As illustrated in Fig. 4c, the $\Delta\delta$ values of XC2 and XC3 in

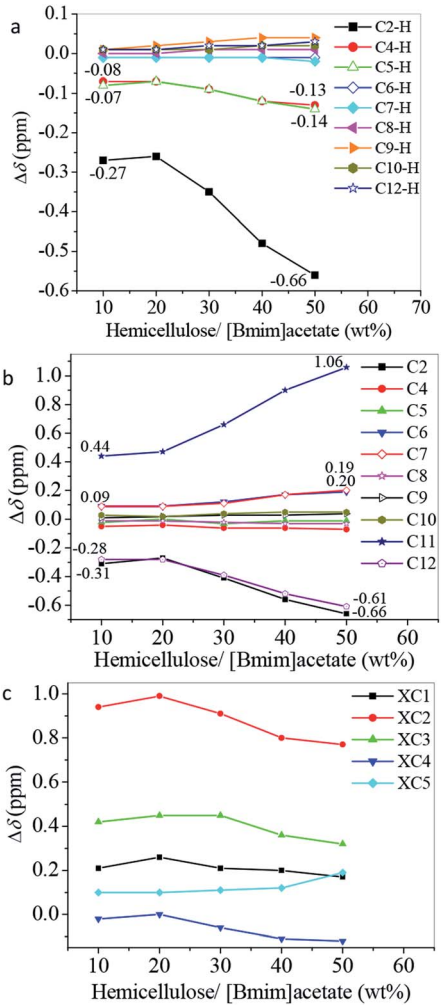

Fig. 4 Relative change of the ^1H and ^{13}C chemical shifts of [Bmim] acetate and hemicellulose as a function of the mass ratio of hemicellulose to [Bmim]acetate referring to the pure [Bmim]acetate and arabinoxylan: (a) relative change of the ^1H chemical shifts of [Bmim] acetate; (b) relative change of the ^{13}C chemical shifts of [Bmim] acetate; (c) relative change of the ^{13}C chemical shifts of the xylopyranose unit in hemicellulose.

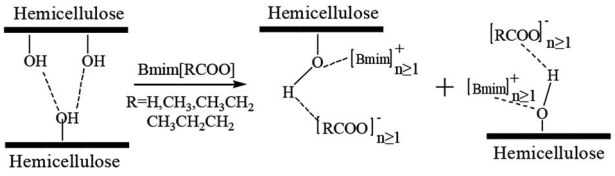

Fig. 5 Proposed dissolution mechanism of bamboo hemicellulose in 1-butyl-3-methylimidazolium carboxylate based ionic liquids.

the xylopyranose unit of hemicellulose decreased with increasing hemicellulose concentration. The interaction strength of the hydroxyl groups at XC2 and XC3 positions with [Bmim]acetate decreased with increasing hemicellulose concentration. The decrease of the relative molecular number of [Bmim]acetate referring to hemicellulose led to the decrease of the average number of IL that interacted with the hydroxyl groups in hemicellulose. This condition resulted in less downfield shift of XC2 and XC3. The hemicellulose concentration had an impact on the hydrogen bond formation between hemicellulose and [Bmim]acetate.

The cation and anion of the ILs played an important role in the hemicellulose dissolution (Fig. 1 and 3). The hemicellulose concentration had a great effect on the hydrogen bond strength between hemicellulose and ILs (Fig. 4). Thus, a possible dissolution mechanism of the bamboo hemicellulose in 1-butyl-3-methylimidazolium carboxylate-based ILs was proposed and depicted in Fig. 5. The acidic proton in imidazolium cation formed a hydrogen bond with a hydroxyl oxygen atom in hemicellulose. Simultaneously, the oxygen atom of the carboxylate anion of ILs interacted with the hydroxyl proton atom in hemicellulose through hydrogen bonding. These hydrogen bonds resulted in the disruption of the inter- and intramolecular hemicellulose, leading to the hemicellulose dissolution in the ILs. However, the hydrogen bond interaction of the hydroxyl oxygen in hemicellulose with acidic proton in the imidazolium cation was much weaker than that of the hydroxyl protons in hemicellulose with carboxylate anion of ILs. The steric effect of these anions may cause a negative effect on the hemicellulose dissolution in ILs. In our earlier report, it is noted that only halide anion attacked hydroxyl proton in hemicellulose to form hydrogen bond, resulting in the dissolution of arabinoxylan-rich hemicellulose from bamboo in 1-butyl-3-methylimidazolium halide-based ILs.[28] Due to the strong electronegativity of the halogen anions, the acidity of the proton in the imidazole cation was very weak, and cannot form hydrogen bonds with the hydroxyl oxygen in the hemicellulose to promote the dissolution of hemicellulose.[28] Or the hydrogen bonds formed between the proton in the imidazole cation and the hydroxyl oxygen in the hemicellulose were very weak.[28] The difference of the interaction mechanism was possibly due to the difference of chemical structure of the anions.

Characterization of the regenerated hemicelluloses from the saturated ILs

Yield, molecular weight, and neutral sugar composition. The hemicelluloses, which were dissolved in the four ILs at the temperature ranging from 120 °C to 150 °C, were regenerated by adding an antisolvent of 95% ethanol. Table 1 presents the yields. Only 53.8–79.2% of hemicelluloses could be recovered from the saturated ILs. This situation is attributed to the hemicellulose with low molecular weight that still remained in the IL solution.

The table also displays the results of molecular weight of the regenerated hemicelluloses. The weight-average molecular weight (M_w), number-average molecular weight (M_n), and polydispersity (M_w/M_n) of the original hemicellulose were approximately 50 200 g mol^{-1}, 39 800 g mol^{-1}, and 1.262, respectively. The regenerated hemicellulose fractions exhibited M_w values varying from 48 600 g mol^{-1} to 52 600 g mol^{-1}. These values were similar with those of the original hemicellulose (50 200 g mol^{-1}). Almost no degradation occurred during the hemicellulose dissolution in the ILs at the temperature ranging from 120 °C to 150 °C. The ILs and temperature showed almost no impact on the M_w values of the hemicellulose. The increase of M_n values varying from 43 600 g mol^{-1} to 49 500 g mol^{-1} resulted in slightly low polydispersities (M_w/M_n, 1.061–1.168) of the regenerated hemicelluloses compared with that of the original hemicellulose (1.262). The possible unregenerated hemicelluloses with low molecular weight led to a uniform molecular weight distribution of the regenerated hemicelluloses than the original hemicellulose.[25,28]

Table 1 summarizes the neutral sugar compositions in the regenerated and original hemicelluloses. No significant differences were documented in the relative content of neutral sugars of the original and regenerated hemicelluloses. This result further suggested that the backbone of hemicellulose was preserved by the ILs during dissolution. The main neutral sugar component of the hemicellulose was almost unchanged. Xylose (73.3–87.6%) was the dominant component sugar in all hemicellulose samples, followed by arabinose (8.2–16.4%). The total content of xylose and arabinose accounted for >81%. Mannose (0.3–11.6%), galactose (0.0–3.9%), and glucose (2.1–8.8%) were present in minor quantities in all hemicellulose samples.

The FT-IR spectra of the original and the representative regenerated hemicelluloses are shown in Fig. 6. Evidently, the FT-IR spectra of the regenerated hemicelluloses were similar to those of the original ones. The main chain of regenerated hemicelluloses was preserved by the ILs during dissolution.[28] Specifically, the ILs only acted as solvent for the dissolution of the bamboo hemicellulose. The characteristic peaks associated with hemicellulose were observed at 3433 cm^{-1} (–OH stretching vibration), 2970 and 2934 cm^{-1} (C–H asymmetrical and symmetrical stretching of –CH_2–, respectively), 1420 cm^{-1} (–CH_2– deformation), 1378 cm^{-1} (C–H bending vibration), 1167 cm^{-1} (C–O–C and C–C stretching), 1250 and 1050 cm^{-1} (C–O stretching or C–OH bending), and 987 and 897 cm^{-1}.[2,8,25,26,28,36] The weak band at 987 cm^{-1} indicated the presence of arabinofuranose unit attached at the O-3 position of the xylopyranosyl constituents.[25,26] The sharp band at 897 cm^{-1} was characteristic of the β-glycosidic linkages among the sugar units.[25,26] The absorption at 1640 cm^{-1} was attributed to the absorbed water.[2] The band at 1510 cm^{-1} was attributed to the aromatic skeletal vibrations; this notion indicated that the

Table 1 Yield, weight-average (M_w) and number-average molecular weights (M_n) and polydispersity (M_w/M_n) of and neutral sugar contents (relative%) in the regenerated and original hemicelluloses[a]

					Neutral sugar contents (relative%)					
Samples	Yields (%)	M_w (g mol^{-1})	M_n (g mol^{-1})	M_w/M_n	Arabinose (Ara)	Xylose (Xyl)	Mannose	Galactose	Glucose	Ara + Xyl (%)
OH_0	—	50 200	39 800	1.262	8.7	87.6	0.9	0.7	2.1	96.3
RH_{1-1}	69.6	52 600	49 500	1.063	8.2	73.3	11.6	3.9	3.0	81.5
RH_{1-2}	60.2	50 500	46 700	1.081	13.9	80.2	1.9	n.d.	4.0	94.1
RH_{1-3}	57.8	51 000	47 500	1.074	14.3	81.8	0.3	0.2	3.5	96.1
RH_{1-4}	56.2	48 600	43 600	1.115	11.3	81.8	1.3	0.0	5.6	93.1
RH_{2-1}	67.7	49 500	44 000	1.125	12.9	78.3	0.8	1.7	6.3	91.2
RH_{2-2}	71.3	49 600	44 500	1.114	11.1	77.8	1.1	1.6	8.5	88.9
RH_{2-3}	61.4	50 400	46 100	1.093	14.1	78.3	1.0	0.9	5.8	92.4
RH_{2-4}	63.0	49 600	45 100	1.100	12.1	79.4	1.1	1.2	6.2	91.5
RH_{3-1}	79.2	51 200	45 700	1.118	10.2	81.3	1.0	1.2	6.4	91.5
RH_{3-2}	59.7	48 800	44 200	1.104	13.6	79.0	1.2	n.d.	6.3	92.6
RH_{3-3}	67.5	51 100	46 900	1.090	9.2	83.6	0.7	0.2	6.3	92.8
RH_{3-4}	60.8	52 000	44 500	1.168	10.4	81.3	1.1	n.d.	7.2	91.7
RH_{4-1}	71.4	52 200	49 100	1.063	11.8	77.2	1.6	1.7	7.6	89.0
RH_{4-2}	59.9	50 500	46 100	1.095	16.4	70.4	2.1	2.3	8.8	86.8
RH_{4-3}	53.8	50 900	47 000	1.083	13.5	78.9	0.7	n.d.	6.9	92.4
RH_{4-4}	56.7	51 200	47 800	1.071	13.6	79.5	0.8	0.2	5.9	93.1

[a] n.d., not determined.

bamboo hemicellulose was slightly contaminated with minimal amounts of bound lignin.[2,28] The bands at 1568 and 1467 cm^{-1} responded to the symmetrical stretching of the carboxylic anions and the bending vibrations of $-CH_3$ and $-CH_2-$,[37] respectively. The regenerated hemicellulose was contaminated with a small amount of ILs. The FT- IR spectra (Fig. 6) and neutral sugar composition (Table 1) indicated that the bamboo hemicellulose has a structural backbone comprising xylan with arabinose as side chain. The results of molecular weight and neutral sugar analyses (Table 1) and the FT-IR spectra (Fig. 6) of the regenerated hemicellulose showed that the structure of bamboo hemicellulose was preserved by the ILs during dissolution. The ILs only served as solvation agents for hemicellulose.

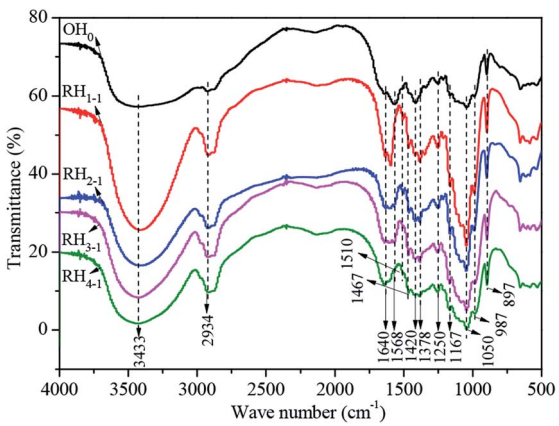

Fig. 6 FT-IR spectra of the original (OH_0) and regenerated hemicelluloses from [Bmim]formate (RH_{1-1}), [Bmim]acetate (RH_{2-1}), [Bmim]propionate (RH_{3-1}), and [Bmim]butyrate (RH_{4-1}) at saturated state at 120 °C.

Conclusions

This study evaluated the solubility of arabinoxylan-rich hemicellulose from bamboo in four ILs by fixing the cation as 1-butyl-3-methylimidazolium but with varying carboxylate anion (formate, acetate, propionate, and butyrate). ^{1}H NMR and ^{13}C NMR techniques were used to investigate the influence of the anionic structure on hemicellulose dissolution. The recovered hemicellulose fractions from the IL solutions were characterized. The hemicellulose solubility increased with increasing temperature in the range of 30–150 °C. The solubility was in the order: [Bmim]acetate > [Bmim]formate > [Bmim]butyrate > [Bmim]propionate. [Bmim]acetate performed a strong ability to dissolve hemicellulose. The acidic protons in 1-butyl-3-methylimidazolium cation formed a hydrogen bond with the hydroxyl oxygen atom in hemicellulose. By contrast, the oxygen atom in the carboxylate anion interacted with the hydroxyl proton in hemicellulose. The hydrogen bond formation between the ILs and hemicellulose resulted in hemicellulose dissolution in the ILs. The interaction strength had an important effect on the solubility. The hydroxyl groups at XC2 position of xylopyranose units of hemicellulose easily formed a hydrogen bond with ILs than those at XC3 position of xylopyranose units. The alkyl chain of the carboxylate anion and the hemicellulose concentration made a great impact on the interaction strength. The hemicellulose was not degraded in the ILs during the dissolving process. The regenerated hemicellulose also exhibited a similar structural feature to the original one. This study would

have important guiding significance for the selection and design of ILs for dissolution of hemicellulose and pretreatment of lignocellulosic biomass.

Experimental section

Materials

Bamboo (*Phyllostachys pubescens* Mazel) from a local forest in Nanchang City (China) was used for extracting hemicellulose. The dried bamboo stem was ground and screened to collect powder with sizes of 40–100 mesh. The powder was then further dried for 12 h at 50 °C in an oven before hemicellulose extraction. [Bmim]formate (99%), [Bmim]acetate (99%), [Bmim] propionate (99%), and [Bmim]butyrate (99%) were purchased from Shanghai Chengjie Chem. Co., Ltd., China. The ILs were further dried in a vacuum oven for 24 h at 150 °C before use. The water content in each IL measured using Karl–Fischer method was <1000 ppm. The schematic structures, numbering, and abbreviations of these four ILs are displayed in Fig. 1. Acetic acid (>99.8%), ethanol (95%), pyridine (99%), and DMSO-d_6 (>99.9%) were purchased from Shanghai Aladdin Chem. Co., Ltd., China. Chlorotrimethylsilane (99%) and 1,1,1,3,3,3-hexamethyldisilazane (99%) were purchased from J&K Scientific Co., Ltd. China. D-(+)-Galactose (>95%), D-(+)-mannose (99%), D-(+)-xylose (99%), D-glucose (>95%), L-(+)-arabinose (99%), and trifluoroacetic acid (99%) were purchased from Heowns Biochemical Technology Co., Ltd., China. These reagents were used as received. Distilled and deionized water was used as the solvent for the preparation of all relative solutions.

Preparation of bamboo hemicellulose

Bamboo hemicellulose was prepared according to the previously reported method with some modifications.[2] First, the dried bamboo flour was extracted with petroleum ether–ethanol (2 : 1, mL mL^{-1}) in a Soxhlet extractor for 12 h at 75 °C to remove the fat, pigment, and wax. Second, the fully dried defatted and dewaxed bamboo flour was treated with 0.6 wt% $NaClO_2$ (adjusted to pH 4.2–4.7 with anhydrous acetic acid) for 6 h at 75 °C under stirring to partially remove lignin and obtain holocellulose. The ratio of dry matter to liquor was 1 : 10 (w/v, g mL^{-1}). Third, the holocellulose was extracted with 5 wt% NaOH for 18 h at 30 °C with the solid–liquid ratio of 1 : 20 (w/v, g mL^{-1}). The alkaline filtrate containing solubilized hemicellulose was adjusted to pH 5.5 with anhydrous acetic acid and settled for 2 h after filtration. The pellet was washed with 70% ethanol for several times after centrifugation and then fully freeze-dried. Finally, the yellow powder of the bamboo hemicellulose, which mainly consists of arabinoxylans,[2] was obtained for further utilization. The schematic structure and numbering of the hemicellulose is shown in Fig. 1.

Measurement of hemicellulose solubility in the ILs

First, the IL (10 g) was sealed in a round-bottomed flask and heated to a designed temperature in an oil bath (DF-101S, Gongyi Yingyu Instrument Factory in China). Thereafter, the completely dried bamboo hemicellulose powder (5 mg) was added. The mixture was heated for 1 h at the designed temperature with continuous magnetic stirring at 200 rpm. The solution was then carefully checked by placing a drop between two clean glass and observing the solution under a fluorescence microscope (LWD200-37FT, Shanghai Dimensional Measurement Factory in China) to justify if hemicellulose particles were undissolved. This procedure was repeated for several times until the additional hemicellulose could not be dissolved further within 1 h. Subsequently, the hemicellulose was judged as becoming saturated. The hemicellulose solubility at the given temperature was defined as the total amount of hemicellulose dissolved in 100 g IL (g/100 g IL). The solubility values of the hemicellulose in the four types of ILs were measured in the temperature range of 30–120 °C with 10 °C intervals.

Nuclear magnetic resonance (NMR) analysis of the mixture of hemicellulose and ILs

In order to elucidate the interaction between hemicellulose and ILs, the changes in ^1H and ^{13}C chemical shifts of the hemicellulose and ILs were obtained through ^1H and ^{13}C NMR techniques, and the hemicellulose concentration was 10 wt% referring to 200 mg ILs in 0.5 mL DMSO-d_6. After the hemicellulose was completely dissolved, the solution was transferred into a 5 mm NMR tube for analysis. As control, 20 mg original hemicellulose and 200 mg IL were dissolved in 0.5 mL DMSO-d_6, respectively. The ^1H NMR spectra were recorded at 600.5 MHz. The ^{13}C NMR spectra were recorded at 100.6 MHz. The relative changes of the chemical shifts were calculated according to eqn (1)–(3). [Bmim]acetate was selected as a representative to elucidate the effect of hemicellulose concentration on the interaction between hemicellulose and ILs. 20–100 mg hemicellulose powder was dissolved in 0.5 mL DMSO-d_6, which contained 200 mg [Bmim]acetate, thereby resulting in 10 wt% to 50 wt% hemicellulose concentration in [Bmim]acetate.

$$\Delta\delta_{IL} = \delta_{IL\ in\ mixture} - \delta_{Pure\ IL} \quad (1)$$

$$\Delta\delta_{Hemicellulose} = \delta_{Hemicellulose\ in\ mixture} - \delta_{Pure\ hemicellulose} \quad (2)$$

$$\Delta\delta_{DMSO\text{-}d_6} = \delta_{DMSO\text{-}d_6\ in\ mixture} - \delta_{DMSO\text{-}d_6\ in\ pure\ IL} \quad (3)$$

Regeneration and characterization of hemicelluloses from saturated IL solution

Regeneration of hemicelluloses. After the saturated IL solution is cooled to room temperature, the saturated IL solution was precipitated with three volumes of 95% (w/w) ethanol under stirring. The mixture was then settled for 12 h before centrifugation at 4000 rpm for 20 min. The collected hemicellulose was repeatedly washed with 95% (w/w) ethanol until the complete removal of IL residue. Finally, the regenerated hemicellulose was fully freeze-dried and used for further characterization.

The hemicellulose fractions regenerated from saturated [Bmim]formate were labeled as RH_{1-1}, RH_{1-2}, RH_{1-3}, and RH_{1-4}, which corresponded with the dissolution temperatures at 120 °C, 130 °C, 140 °C, and 150 °C, respectively. The samples regenerated from saturated [Bmim]acetate at dissolution temperatures of

120 °C, 130 °C, 140 °C, and 150 °C were marked as RH_{2-1}, RH_{2-2}, RH_{2-3}, and RH_{2-4}, respectively. The hemicellulose fractions regenerated from saturated [Bmim]propionate were labeled as RH_{3-1}, RH_{3-2}, RH_{3-3}, and RH_{3-4}, corresponding to the dissolution temperatures at 120 °C, 130 °C, 140 °C, and 150 °C, respectively. The hemicellulose samples isolated from saturated [Bmim] butyrate were labeled as RH_{4-1}, RH_{4-2}, RH_{4-3}, and RH_{4-4}, corresponding with the dissolution temperatures at 120 °C, 130 °C, 140 °C, and 150 °C, respectively. The original hemicellulose was also labeled as OH_0.

Characterization of hemicelluloses

The average molecular weights (M_W) of the hemicellulose samples were estimated by gel permeation chromatography (1200 Series, Agilent Corporation, USA) on a PL aquagel-OH MIXED column (7.5 mm × 300 mm, Agilent Corporation, USA), calibrated with dextran (Sigma-Aldrich) standards with M_W of 1270, 5220, 11 600, 23 800, and 48 600. The eluent was 0.005 M sodium phosphate buffer (containing 0.02 wt% NaN_3) with the pH value of 7.5. The injection volume was 100 μL, the flow rate was 0.5 mL min^{-1}, and the column oven temperature was maintained at 30 °C. Before injection, all hemicellulose samples were dissolved in 0.005 M sodium phosphate buffer at a concentration of 0.1 wt% and then filtered through a 0.22 μm microporous cellulose membrane.

The neutral sugar compositions of the original and regenerated hemicelluloses were determined according to a previously reported method with some modifications.[29] Hemicellulose (20 mg) was completely hydrolyzed with 3.0 M trifluoro acetic acid at 120 °C for 3 h in a 30 mL pressure vessel. Afterward, the anhydrous ethanol was added into the hydrolysate. Subsequently, the residues of trifluoro acetic acid and water were removed with a rotary vacuum evaporator at 55 °C. This procedure was repeated several times to ensure complete removal of trifluoro acetic acid and water. Subsequently, the dried hydrolysate was completely dissolved in 2.0 mL anhydrous pyridine at 50 °C. Thereafter, 0.8 mL chlorotrimethylsilane and 1.6 mL 1,1,1,3,3,3-hexamethyldisilazane were added into the pyridine solution and maintained at 50 °C for 1 h. After dehydration by adding anhydrous Na_2SO_4, the supernatant liquid was analyzed by gas chromatography-mass spectrometry (GC-MS) 7890B-7000D (Agilent Corporation, USA) on a HP-PONA (Agilent Corporation, USA) capillary column (50 m × 200 μm × 0.5 μm). Approximately 1 μL sample was automatically injected, and highly purified He with a flow rate of 15 mL min^{-1} was used as a carrier gas with a split ratio of 50 : 1. The mass spectra were obtained by electron impact ionization at 70 eV. The oven temperature was programmed as follows: (1) hold at an initial temperature of 45 °C for 5 min, (2) from 45 °C to 180 °C at an increment of 5 °C min^{-1} and hold at 180 °C for 2 min, (3) from 180 °C to 280 °C with a heating rate of 8 °C min^{-1} and then hold at 280 °C for 3 min. The standard sugar, including D-(+)-galactose), D-(+)-mannose, D-(+)-xylose, D-glucose, and L-(+)-arabinose, was also silylated and analyzed by GC-MS.

The Fourier transform infrared spectroscopy (FT-IR) of the original and regenerated hemicelluloses were obtained on a Nicolet is5 FT-IR spectrophotometer (Thermo Fisher Scientific Corporation, USA) with KBr pellets in the range of 4000–400 cm^{-1} at 2 cm^{-1} resolution.

Conflicts of interest

There are no conflicts to declare.

Acknowledgements

This work was financially supported by the National Natural Science Foundation of China (No. 21666022).

Notes and references

1 N. B. Appiah-Nkansah, J. Li, W. Rooney and D. Wang, *Renew. Energy*, 2019, **143**, 1121–1132.
2 H. Peng, N. Wang, Z. R. Hu, Z. P. Yu, Y. H. Liu, J. S. Zhang and R. Ruan, *Ind. Crop. Prod.*, 2012, **37**(1), 41–50.
3 B. M. Matsagar and P. L. Dhepe, *New J. Chem.*, 2017, **41**(14), 6137–6144.
4 T. Y. Chen, B. Wang, Y. Y. Wu, J. L. Wen, C. F. Liu, T. Q. Yuan and R. C. Sun, *Int. J. Biol. Macromol.*, 2017, **101**, 747–757.
5 E. Peduzzi, G. Boissonnet, G. Haarlemmer and F. Maréchal, *Sustainable Energy Fuels*, 2018, **2**(5), 1069–1084.
6 P. Karagoz, R. M. Bill and M. Ozkan, *Renew. Energy*, 2019, **143**, 741–752.
7 H. Peng, A. S. Yang and J. H. Xiong, *Carbohydr. Polym.*, 2013, **91**(1–2), 348–355.
8 G. H. Yang, H. F. Zhou, J. C. Chen, G. J. Lyu, Y. Y. Xia and L. A. Lucia, *Int. J. Mol. Sci.*, 2017, **18**(12), 2502–2513.
9 A. Mazar, N. Jemaa, W. W. Al Dajani, M. Marinova and M. Perrier, *Biomass Bioenergy*, 2018, **111**, 103–113.
10 B. M. Matsagar and P. L. Dhepe, *Catal. Sci. Technol.*, 2015, **5**(1), 531–539.
11 R. Acosta, J. Sanabria and D. Nabarlatz, *Chem. Eng. Trans.*, 2018, **65**, 667–672.
12 J. C. López-Linares, I. Romero, C. Cara, E. Castro and S. I. Mussatto, *Bioresour. Technol.*, 2018, **247**, 736–743.
13 M. J. Cocero, Á. Cabeza, N. Abad, T. Adamovic, L. Vaquerizo, C. M. Martínez and M. V. Pazo-Cepeda, *J. Supercrit. Fluids*, 2018, **133**, 550–565.
14 A. K. Kumar and S. Sharma, *Bioresour. Bioprocess.*, 2017, **4**(1), 7–26.
15 R. B. Stoffel, P. V. Neves, F. E. Felissia, L. P. Ramos, L. M. Gassa and M. C. Area, *Biomass Bioenergy*, 2017, **107**, 93–101.
16 Y. J. Cao, R. B. Zhang, T. Cheng, J. Guo, M. Xian and H. Z. Liu, *Appl. Microbiol. Biotechnol.*, 2017, **101**(2), 521–532.
17 K. E. Gutowski, *Phys. Sci. Rev.*, 2018, **3**(5), 1–10.
18 P. A. Thomas and B. B. Marvey, *Molecules*, 2016, **21**(2), 184–200.
19 P. Reddy, *S. Afr. J. Sci.*, 2015, **111**(11–12), 1–9.
20 K. C. Badgujar and B. M. Bhanage, *Bioresour. Technol.*, 2015, **178**, 2–18.
21 K. Dong, S. H. Zhang and J. J. Wang, *Chem. Commun.*, 2016, **52**(41), 6744–6764.

22 Y. Li, J. J. Wang, X. M. Liu and S. J. Zhang, *Chem. Sci.*, 2018, **9**(17), 4027–4043.
23 A. R. Xu, Y. B. Zhang, W. W. Lu, K. S. Yao and H. Xu, *J. Mol. Liq.*, 2014, **197**, 211–214.
24 W. E. Hart, J. B. Harper and L. Aldous, *Green Chem.*, 2015, **17**(1), 214–218.
25 X. W. Peng, J. L. Ren and R. C. Sun, *Biomacromolecules*, 2010, **11**(12), 3519–3524.
26 H. Y. Li, X. Chen, Y. J. Li, X. F. Cao, S. N. Sun and R. C. Sun, *Sep. Purif. Technol.*, 2018, **191**, 364–369.
27 P. Moyer, M. D. Smith, N. Abdoulmoumine, S. C. Chmely, J. C. Smith, L. Petridis and N. Labbé, *Phys. Chem. Chem. Phys.*, 2018, **20**(4), 2508–2516.
28 L. Yuan, H. Peng, L. F. Hu, R. B. Yu, W. Y. Peng, R. Ruan, Q. Xia, Y. Zhang and A. H. Liu, *BioResources*, 2019, **14**(1), 2097–2112.
29 Q. T. Chen, A. R. Xu, Z. Y. Li, J. J. Wang and S. J. Zhang, *Green Chem.*, 2011, **13**(12), 3446–3452.
30 Y. J. Zhang, A. R. Xu, B. L. Lu, Z. Y. Li and J. J. Wang, *Carbohydr. Polym.*, 2015, **117**, 666–672.
31 A. Pinkert, K. N. Marsh, S. Pang and M. P. Staiger, *Chem. Rev.*, 2009, **109**, 6712–6728.
32 K. C. Badgujar and B. M. Bhanage, *Bioresour. Technol.*, 2015, **178**, 2–18.
33 B. L. Lu, A. R. Xu and J. J. Wang, *Green Chem.*, 2014, **16**(3), 1326–1335.
34 A. S. Gross, A. T. Bell and J. W. Chu, *J. Phys. Chem. B*, 2011, **115**(46), 13433–13440.
35 A. R. Xu and Y. B. Zhang, *J. Mol. Liq.*, 2015, **1088**, 101–104.
36 X. H. Zhao, T. T. Tong, H. L. Li, H. J. Lu, J. L. Ren, A. P. Zhang, X. Y. Chen and A. M. Wu, *Carbohydr. Polym.*, 2017, **156**, 333–339.
37 Y. Y. Jiang, C. Guo, H. S. Xia, I. Mahmood, C. Z. Liu and H. Z. Liu, *J. Mol. Catal. B: Enzym.*, 2009, **58**(1–4), 103–109.